

Communication

Highly Responsive, Miniaturized Methane Telemetry Sensor Based on Open-Path TDLAS

Qi Wu ¹, Yuanjin Yang ¹, Yuechun Shi ^{2,3}, Yang Xu ¹, Wenlong Wang ², Chao Men ² and Bingxiong Yang ^{1,4,*}

¹ College of Mechanical & Electrical Engineering, Nanjing University of Aeronautics and Astronautics, Nanjing 210016, China

² Nanjing Puguang Chip Technology Co., Nanjing 211800, China

³ Precision Photonics Integration Research Center Yongjiang Laboratory, Ningbo 315202, China

⁴ Jiangsu Jicui Precision Manufacturing Research Institute, Nanjing 211805, China

* Correspondence: bingxy@nuaa.edu.cn

Abstract: This paper proposes the design of a highly responsive, compact, non-contact methane telemetry sensor, employing the open-path tunable diode laser absorption spectroscopy (OP-TDLAS) technology. The sensor uses the dual-core structure of FPGA and ARM to achieve high-speed methane telemetry at 100 KHz repeated modulation frequency for the first time with a non-cooperate target, and a higher gas responsive time of 1.8 ms was achieved than previously reported. Moreover, the optical system (L × W × H: 68.8 × 52 × 62.7 mm) and the electronic system (L × W: 70 × 50 mm) make the sensor more compact. Methane gas samples of varying integral concentrations were examined at a distance of 20 m. The amplitude of the absorption peaks was subjected to a linear fit with the standard concentration values, resulting in a robust linear correlation coefficient ($R^2 = 0.998$). Notably, despite the compact form factor of the methane sensor, it demonstrated commendable stability in gas concentration detection, offering a minimum detection limit of 43.14 ppm·m. Consequently, this highly responsive and compact methane sensor, with its open-path feature, is apt for integration into a variety of applications requiring such attributes. These include handheld telemetry devices, Unmanned Aerial Vehicle (UAV) gas detection systems, vehicle mounted gas detection, and laser gas radar.

Keywords: high responsiveness; miniaturization; methane telemetry; OP-TDLAS



Citation: Wu, Q.; Yang, Y.; Shi, Y.; Xu, Y.; Wang, W.; Men, C.; Yang, B.

Highly Responsive, Miniaturized Methane Telemetry Sensor Based on Open-Path TDLAS. *Photonics* **2023**, *10*, 1281. <https://doi.org/10.3390/photonics10111281>

Received: 30 August 2023

Revised: 12 November 2023

Accepted: 17 November 2023

Published: 19 November 2023



Copyright: © 2023 by the authors. Licensee MDPI, Basel, Switzerland. This article is an open access article distributed under the terms and conditions of the Creative Commons Attribution (CC BY) license (<https://creativecommons.org/licenses/by/4.0/>).

1. Introduction

Methane, a highly flammable and explosive gas, is a significant component of natural gas and biogas, which is commonly encountered in industrial settings such as oil fields and mines. When the concentration of leaked methane mixed with air reaches the flammable limit range, it can trigger safety incidents such as explosions and fires, causing severe injuries and economic losses. Additionally, methane is a powerful greenhouse gas, with a greenhouse effect approximately 25 times higher than that of carbon dioxide per unit mass, and has a significant impact on the global climate. High concentrations of methane can also contribute to air pollution, which is hazardous to human health. Therefore, timely monitoring of methane concentrations and rapid localization of leaks are crucial for environmental protection, air quality maintenance, industrial accident prevention, and personal safety risk reduction [1–4].

Traditional gas concentration detection methods typically employ electrochemical and catalytic combustion approaches, which are hampered by limitations such as poor long-term stability, slow response times, short lifespan, and potential hazards. Unlike the above methods, laser gas spectroscopy relies on detecting the spectral absorption lines of gas molecules, which are highly fingerprint selective, sensitive and allow non-contact measurement. Laser gas detection techniques such as photoacoustic spectroscopy, light-induced thermoelastic spectroscopy, Raman spectroscopy, and laser absorption spectroscopy are

currently gaining a lot of attention in the field of sensing. Ziting Lang et al. demonstrated the heterodyne light-induced thermoelastic spectroscopy (H-LITES) technique, based on Fabry–Pérot (F-P) phase demodulation for acetylene gas measurement, for the first time [5]. Chu Zhang et al. proposed a gas sensor based on differential quartz-enhanced photoacoustic spectroscopy, which showed good performance [6]. However, these gas detection technologies often have complex system structures, high costs, and slow response times. Their existing status as laboratory-stage technologies hinders the integration and commercialization of gas sensors, consequently limiting sensor applications. In contrast, a variant of laser absorption spectroscopy, known as tunable diode laser absorption spectroscopy (TDLAS), has seen rapid development in gas detection methods due to its simple system structure, high sensitivity, and minimal environmental influence. O. Witzel et al. reported the first application of a vertical-cavity surface-emitting laser (VCSEL) for calibration- and sampling-free, high-speed, in situ H₂O concentration measurements in IC engines using direct TDLAS [7]. Chang Liu et al. developed a fan-beam tomographic sensor using tunable diode lasers capable of simultaneously imaging temperature and gas concentration with high spatial and temporal resolutions [8]. Gas concentration detection based on TDLAS is usually categorized by gas chamber type into fixed-point measurement with fixed optical path structure and non-cooperative target gas telemetry with open optical path. The former often requires a fixed gas chamber and a fixed reflective surface, making it challenging to be adapted to gas telemetry, where no fixed reflective surface is required. Therefore, the remote gas telemetry technology based on open-path TDLAS (OP-TDLAS) has been the subject of numerous scholarly investigations because of its capability for handling a long-distance, non-cooperative target [9–12]. Hongbin Lu et al. designed a real-time gas concentration detection system under open optical path conditions, and the experiments showed that gas detection performance was excellent; however, the response time was 2.79 s [13]. Haoqing Yang et al. implemented a digital lock-in amplifier to extract $1f$ and $2f$ signals of wavelength modulated spectra (WMS) using FPGA, and a $2f/1f$ method was adopted to eliminate the influence of ambient light to detect methane concentration; the response time of the designed methane telemetry sensor was 2.5 s [14]. Shuqian Shen et al. proposed a modified $WMS - 2f/1f$ method to improve the stability of the methane telemetry system, which showed good performance with a response time of 0.57 s at a distance of 10 m [15]. However, these gas telemetry sensors implement WMS and lock-in amplifiers to optimize gas sensitivity, leading to disadvantages such as slow response speed, large sensor size, and high cost [16,17]. These factors make it challenging for these sensors to adapt to the field of high-speed gas measurements for purposes such as UAV gas detection, vehicle-mounted detection, and handheld telemetry devices. In contrast, direct absorption spectroscopy (DAS) facilitates faster scanning of gas absorption peaks, enabling high-speed responsiveness in gas sensors. Mohsin Raza et al. used a DAS technique to achieve MHz scanning of a distributed feedback (DFB) laser at 2.3 μm for CO gas measurement [18]. However, their related experiments were conducted under fixed reflector conditions and the system components were relatively large in size, lacking sensor integration and practical application. Therefore, it is important to conduct research on compact gas sensors with high-speed scanning characteristics and open optical paths for practical applications.

In order to solve these problems, we present the design of a highly responsive, compact methane telemetry sensor based on OP-TDLAS. The sensor adopts a dual-core structure of ARM and FPGA, realizing a scanning frequency of 100 KHz for the first time with a non-cooperate target, with a response time of 1.8 ms, far exceeding what has been previously reported. This means that it enables high-speed measurement of methane and rapid location of leakage points. The DAS method not only results in a compact-sized sensor, but also significantly reduces the computational complexity. The experiments validate the sensor's advantages, including its high response speed, strong linearity, and robust stability. Therefore, it is well-suited for applications that demand stringent requirements in

terms of dimension, cost, response speed, and stability. These applications include UAV gas detection, vehicle-mounted detection systems, and handheld telemetry devices.

2. Materials and Methods

2.1. Principle of Direct Absorption Spectroscopy

When a laser beam of length L passes through a uniform gas to be measured, its transmitted light intensity can be expressed by the Lambert–Beer law [19–21], Equation (1):

$$I_t(\nu) = I_0(\nu)e^{-\alpha(\nu)} = I_0(\nu)e^{-PS(T)\varphi(\nu)CL} \tag{1}$$

where $\alpha(\nu)$ is the gas absorption coefficient; $I_0(\nu)$ is the initial light intensity of the laser; $I_t(\nu)$ is the transmitted intensity after passing through the gas; $P(\text{atm})$ is the gas pressure; $S(T)$ ($\text{cm}^{-2}\cdot\text{atm}^{-1}$) is the temperature-dependent absorption intensity of the gas molecules; C is the gas concentration; L (cm) is the optical path length of gas; and $\varphi(\nu)$ is the line-shape function of the gas, under standard conditions of gas temperature and pressure. The line-shape function $\varphi(\nu)$ [22–24] can be expressed as a Lorentz function as follows:

$$\varphi(\nu) = \frac{1}{2\pi} \frac{\gamma_a}{(\nu - \nu_a)^2 + (\frac{\gamma_a}{2})^2} \tag{2}$$

$$\varphi(\nu_a) = \frac{2}{\pi\gamma_a} \tag{3}$$

where γ_a is the full width at half maximum of the absorption line, which is related to the temperature T and the pressure P ; ν_a is the center frequency of the laser; and $\varphi(\nu)$ is a normalized function whose integral over the entire frequency domain satisfies:

$$\int_{-\infty}^{+\infty} \varphi(\nu)d\nu = 1 \tag{4}$$

The gas concentration C can be obtained from Equations (1) and (4):

$$C = \frac{-\ln \frac{I_t(\nu)}{I_0(\nu)}}{PS(T)\varphi(\nu)L} = \frac{\int_{-\infty}^{+\infty} -\ln \frac{I_t(\nu)}{I_0(\nu)}}{PS(T)L} \tag{5}$$

According to Equations (1)–(3), the gas concentration C can also be expressed as:

$$C = \frac{-\ln \frac{I_t(\nu_a)}{I_0(\nu_a)}}{PS(T)\varphi(\nu_a)L} \tag{6}$$

Therefore, based on the above analysis, the gas concentration can be solved by both Equations (5) and (6). In the experiment, the modulation frequency of the laser is in a finite spectral range, so Equation (6) is used for the calculation of the gas concentration.

2.2. The Selection of CH₄ Absorption Lines

For methane telemetry sensors, the methane gas absorption lines need to be selected to minimize interference from other gas absorption spectra. Based on the HITRAN database [25–28], it is known that H₂O and CO₂ in atmospheric gases are the main interfering factors for CH₄ detection errors. Figure 1 displays the integrated concentration values of three gases within the wave number range of 6000–6100 cm^{-1} , when $T = 298.15$ K, $P = 1$ atm, and $L = 100$ cm. In this context, the integral concentrations of H₂O and CO₂ amount to 100,000 ppm·m, whereas the integral concentration of CH₄ is 100 ppm·m. Therefore, it can be seen from the figure that both interfering gases have little effect on the absorption interference of methane in this band. Moreover, for CH₄ molecules, there are three strong absorption peaks in the 6040–6080 cm^{-1} band with the center wave numbers of 6047 cm^{-1} , 6057 cm^{-1} , and 6077 cm^{-1} . Theoretically, lasers with the center wave number

in this band could be used, but in practical applications, the laser with wave numbers of 6057 cm^{-1} and 6077 cm^{-1} have secondary absorption peaks at high concentrations, resulting in methane concentration detection errors. Hence, the DFB laser with a center wave number of 6047 cm^{-1} (1653.7 nm) was selected as the light source of the methane telemetry sensor in this paper.

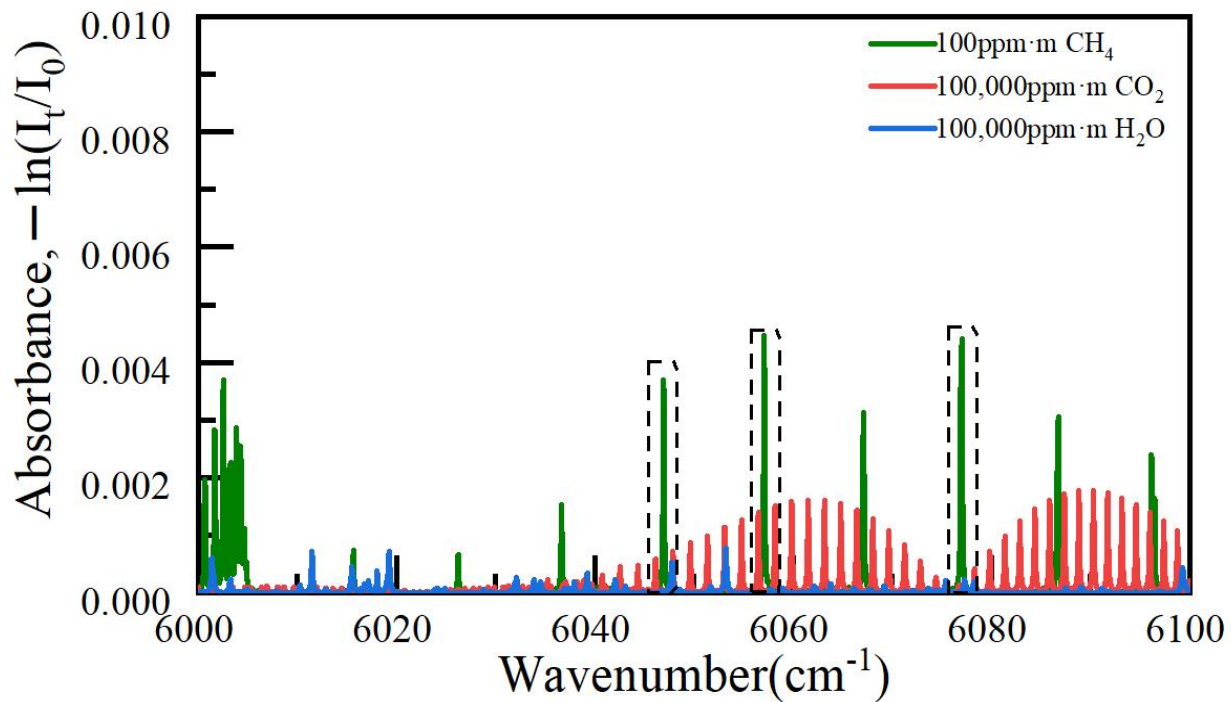


Figure 1. Gas absorption coefficients of H_2O , CO_2 , and CH_4 in the spectral range of $6000\text{--}6100\text{ cm}^{-1}$ from the HITRAN database.

2.3. Experimental Configuration

The methane telemetry sensor is mainly composed of two parts, an optical system and an electronic system, and its overall block diagram is shown in Figure 2. The optical system mainly contains the DFB laser, collimator, and photodiode. The DFB laser (EP-1654-DM, Eblana Photonics, Dublin, Ireland) operates at a central wavelength of 1653.7 nm and is set at an operating temperature of $30\text{ }^\circ\text{C}$. The output light from the laser is passed through a collimator (ACL108U, Thorlabs Inc., Newton, NJ, USA) to produce a collimated laser beam, serving as the gas absorption source. At the signal receiving end, an InGaAs PIN infrared photodiode (G12181-005K, Hamamatsu Photonics K.K., Shizuoka, Japan) and an optical lens ($D = 30\text{ mm}$, $f = 50\text{ mm}$) are used with a pre-amplifier circuit to convert the optical signal containing gas concentration information into an electrical signal for subsequent circuit processing. Furthermore, due to the presence of optical noise from the surrounding environment along with the effective optical signal, a narrow bandpass filter is integrated. This filter is employed to eliminate extraneous light that falls outside the desired target wavelength range. Its purpose is to minimize optical noise, thereby enhancing the telemetry system's signal-to-noise ratio. Simultaneously, a green laser with a wavelength of 520 nm functions as the indicator light source for the entire system. This green laser aids in pinpointing the exact location of the testing point. The configuration of the actual optical system is depicted in Figure 3a.

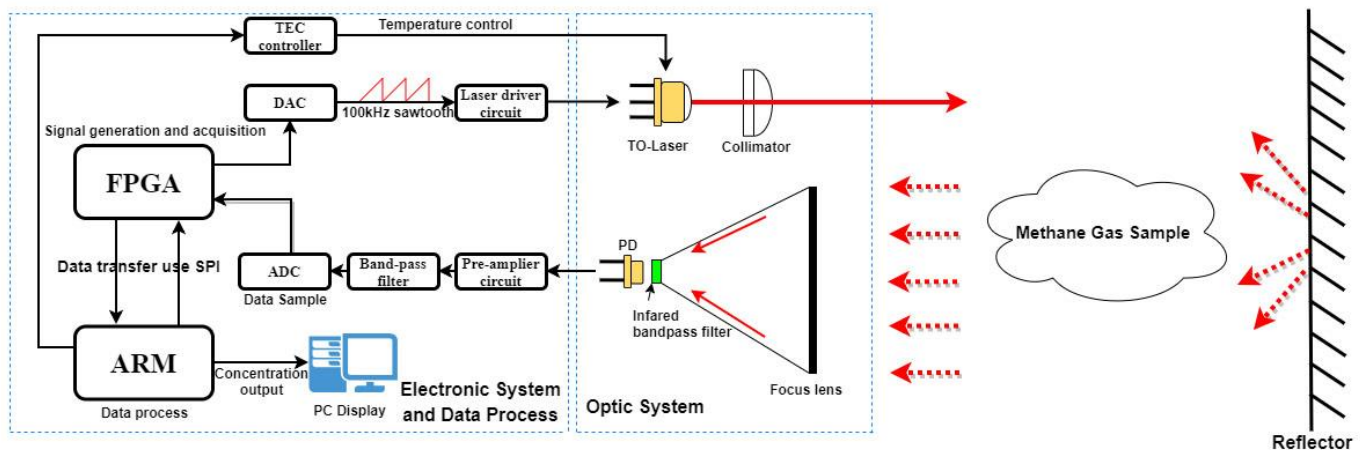


Figure 2. Overall block diagram of the methane telemetry sensor, including the optical and electronic systems.

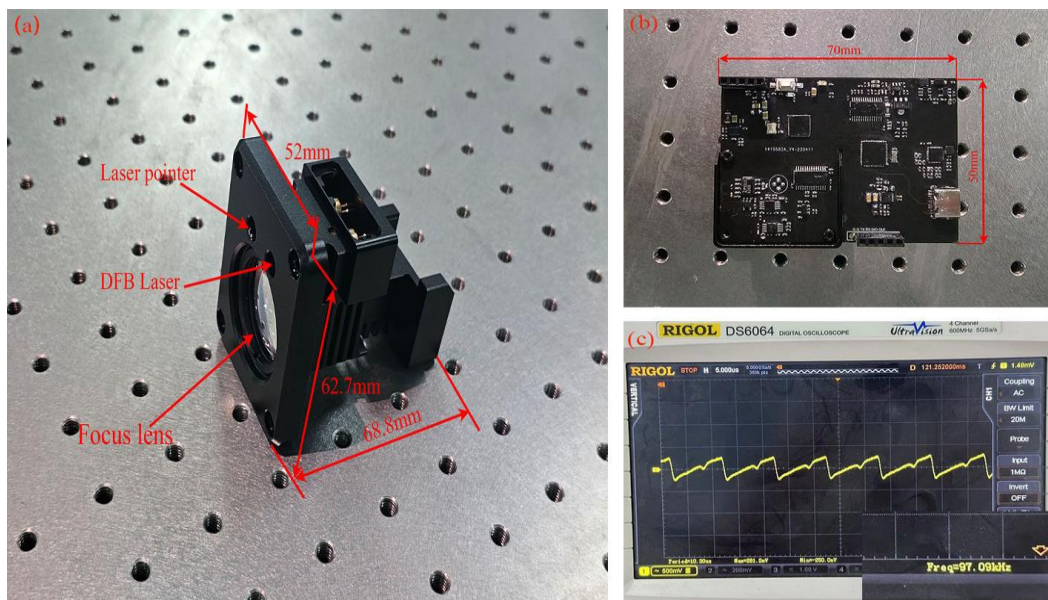


Figure 3. (a) Optical system and dimensions of the methane telemetry sensor. (b) Appearance of the electronic system of the methane telemetry sensor. (c) Reflected wave image with concentration information.

The electronic system is composed of the main control circuit, the laser driver circuit, the TEC temperature control circuit, and the optical signal amplifier circuit, as shown in Figure 3b below. In order to achieve higher response speed and increased scanning frequency of the DFB laser, the main control system uses the dual-core architecture of FPGA (GW1N-LV9QN48C6I5) and ARM (STM32G431CBU6). FPGA generates a 100 KHz high frequency sawtooth signal by controlling a high-speed DAC (AD9760) driver circuit to scan the methane gas absorption line. Because the laser is a current-controlled device, so the modulated drive of the laser is realized through a voltage-controlled constant current source circuit with a current range from 95 to 135 mA. The temperature control circuit achieves negative feedback adjustment of temperature through proportional–integral–derivative control (PID), so the working temperature of the laser can realize fast and long-term stable maintenance at the center wavelength, and the temperature control accuracy can reach ± 0.1 °C. The reflected light passes through the pre-amplifier circuit to realize photoelectric conversion. In order to obtain an effective signal with a higher signal-to-noise ratio, its electrical signal is passed through a second-order bandpass filter circuit to remove noise

from the signal. The signal acquisition circuit uses an ADC (AD9214-65) driver circuit to sample and quantize the filtered signal. Its reflected wave signal with concentration information is shown in Figure 3c, and the concentration signal waveform can be clearly seen, with a laser scanning frequency of 100 KHz. Then, the FPGA buffers the data from the ADC chip using first-in–first-out (FIFO) and sends the raw data to the STM32 processor via a serial peripheral interface (SPI). As the ADC collects data even after the analog filter circuit, it is always accompanied by electronic noise and ADC sampling error, which can increase the error of concentration. Thus, the STM32 uses average filtering on the collected data to eliminate high frequency noise on the data. The unabsorbed portion of the data is then used to fit the background baseline to derive the gas absorption coefficient curve and calculate methane concentration. Finally, the STM32 sends the concentration value to a PC for display via universal asynchronous receiver transmitter (UART) communication.

3. Results

3.1. The Calibration Experiments of Methane Telemetry Sensors

In order to evaluate the linear performance of the methane telemetry sensor, calibration experiments were performed. Using an accurate gas flow meter, gas bags with different CH₄ concentrations were proportioned for calibration experiments using a mixture of CH₄ and N₂. The thickness of the gas bag was 15 cm, so the effective absorption length of gas was 0.15 m. The gas sample to be measured was selected from seven different integral concentrations of gas bags, including pure N₂, 450 ppm·m, 1500 ppm·m, 2550 ppm·m, 3600 ppm·m, 4500 ppm·m, and 7500 ppm·m for calibration experiments at a distance of 20 m. The gas bag was fixed to the wall, using the wall as a reflective surface, where the N₂ was used as a background signal for reference to ensure the accuracy of the methane absorption signal. Figure 4a shows the gas absorption signal for different integral concentrations, obtained by fitting a straight line to the data of the unabsorbed part using the least squares method for a single cycle at the laser scanning frequency of 100 KHz. Amp_{p-p} is used to represent the amplitude of the absorption peak of the gas absorption signal. The linear relationship between the amplitude of the absorption signal Amp_{p-p} and the standard concentration for different integral concentrations is shown in Figure 4b. A linear fit using the experimental data can be expressed as:

$$C = 5.08 \times 10^4 \text{ Amp}_{p-p} - 57.88(\text{ppm}\cdot\text{m}) \tag{7}$$

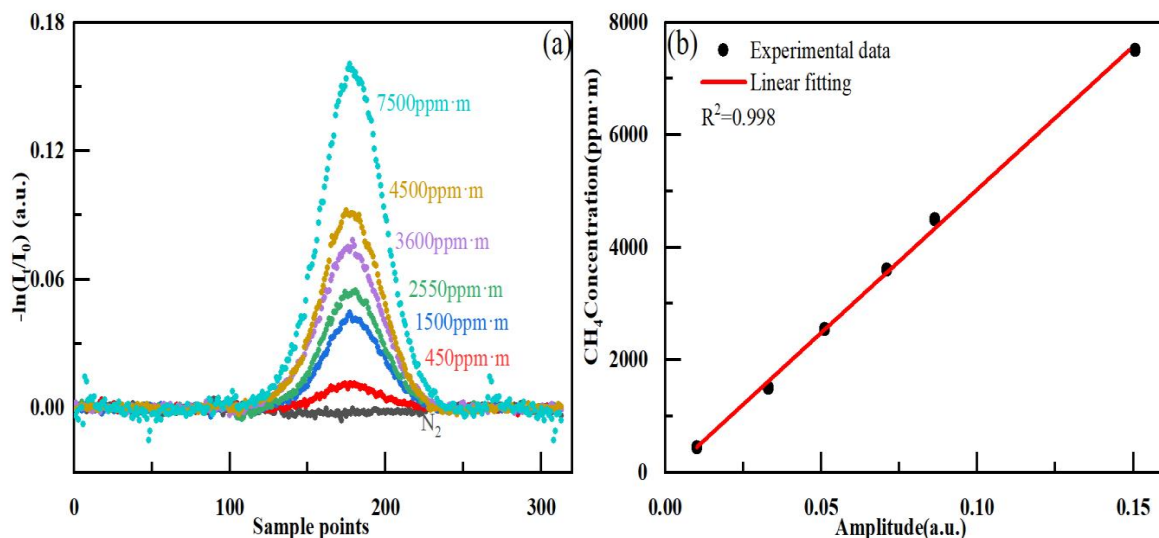


Figure 4. (a) Gas absorption signal after subtracting background baseline for different methane concentrations. (b) Linear correlation of methane gas concentration with Amp_{p-p}.

The linear correlation coefficient between Amp_{p-p} and gas concentration is $R^2 = 0.998$, signifying a strong linear correlation between the amplitude of the absorption signal from this methane telemetry sensor and the methane gas concentration. This correlation validates the method’s accuracy in calculating the concentration.

3.2. Stability and Minimum Limit Experiments

In order to test the concentration stability and minimum detection limit of this methane telemetry sensor, a long-term monitoring experiment was conducted on a methane gas bag with an integrated concentration of 450 ppm·m fixed to a wall at a distance of 20 m. Since the modulation frequency of the laser was 100 KHz, so the amount of detection data per unit time was large. For conducting long-term stability experiments more accurately, the UART communication rate of STM32 was modified so that it output a concentration value in 1 s and the continuous monitoring time was 2100 s. The results are shown in Figure 5. It can be seen that the gas concentration fluctuated in the range of -15 ppm·m to 20.3 ppm·m, indicating that this methane telemetry sensor has excellent long-term stability and can be used for long-term monitoring of methane concentration. As shown in Figure 6, the amplitude of the absorbed signal Amp_{p-p} is 0.012 and the value of $1-\sigma$ for the unabsorbed part of the background noise was 1.15×10^{-3} . Therefore, the signal-to-noise ratio of 10.43 for this methane sensor can be obtained from the ratio of the amplitude of the absorbed signal to the $1-\sigma$ background noise. Therefore, the minimum detection limit of the sensor was 43.14 ppm·m.

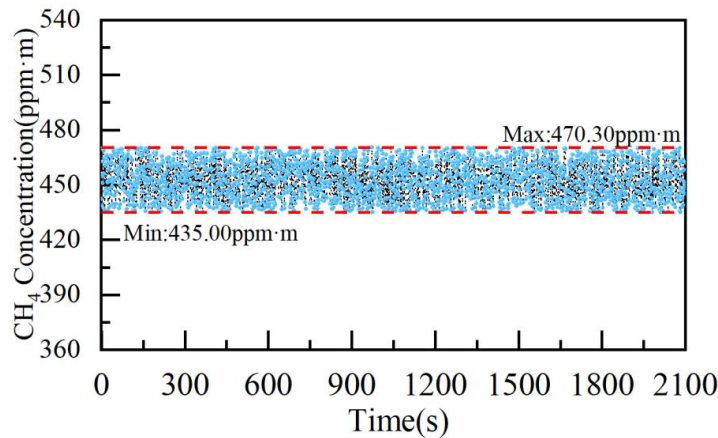


Figure 5. Long-term stability monitoring of the methane telemetry sensor at concentration of 450 ppm·m.

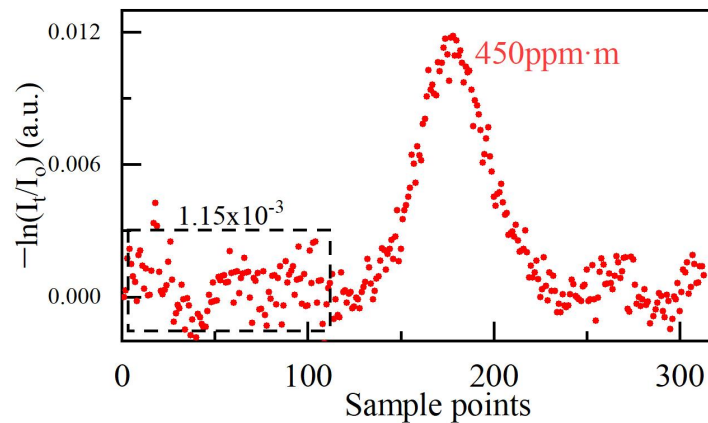


Figure 6. Gas absorption signal for CH₄ concentration of 450 ppm·m.

3.3. Response Time Experiment

To verify the dynamic performance of this methane telemetry sensor, a related responsiveness experiment was conducted using a response time test system (Dalian Aike Science & Technic Development T Co., Ltd., Dalian, China) as shown in Figure 7a below. The gas bag containing the integrated concentration of 3600 ppm·m methane gas was placed in the gas chamber box shown in Figure 7b with a wooden board inside as a reflective surface, which controlled the exposed width of the gas bag, so the exposed width of the gas bag was set to 20 cm. Due to the divergence of the laser beam with increasing distance, which can impact the accuracy of the concentration responsivity experiment, the gas chamber was positioned 6 m away. This ensures that the laser beam spot remains small enough to cover the 20 cm wide gas bag. Then, the methane telemetry sensor was mounted on the rotating platform of the response test system, as shown in Figure 7c, with the platform rotation speed set to 12 r/min. This resulted in an angular speed of 0.4π rad/s for the methane telemetry sensor. It was calculated that the time for the laser light source to pass through the 20 cm wide gas bag was 25 ms, and it took 5 s for one full rotation. The number of rotations was set to 3, making the total measurement time for this experiment 15 s. The response time measurement result is shown in Figure 8a. The response time of the methane telemetry sensor was defined as the time it takes to rise from 10% to 90% of the target concentration, as shown in the red marked area of Figure 8a, its enlarged view is shown in Figure 8b. The average value obtained from three measurements was 1.8 ms. Hence, this methane telemetry sensor demonstrated excellent dynamic responsiveness.



Figure 7. (a) Responsiveness experimental test system. (b) Air box with controllable air bag width. (c) Rotating platform of the responsiveness test system.

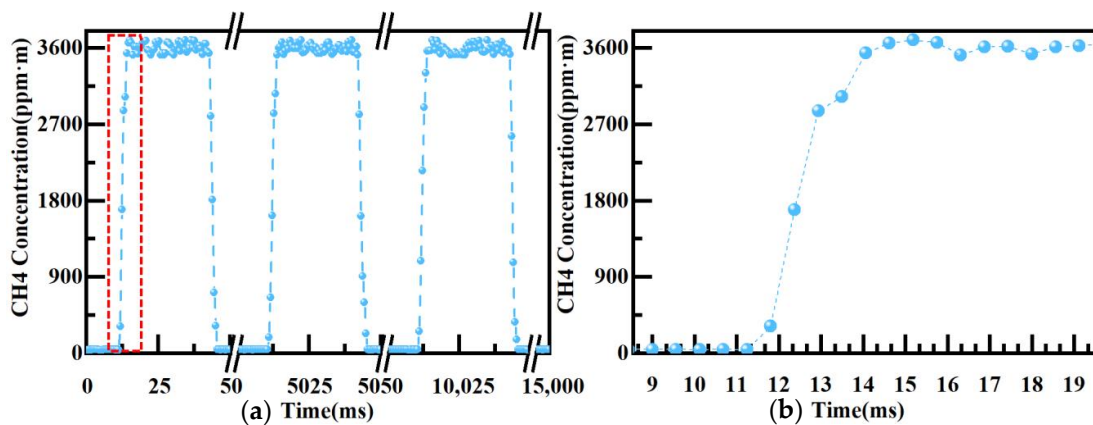


Figure 8. (a) Dynamic responsiveness experiment of methane telemetry sensor. (b) Single transition from 10% to 90% for dynamic responsiveness experiment.

4. Conclusions

In this paper, a highly responsive, compact, non-contact methane telemetry sensor was designed and implemented based on OP-TDLAS. The sensor is compact in size; the dimensions of its optical system are $L \times W \times H$: 68.8 × 52 × 62.7 mm, and the dimensions of its circuit system are $L \times W$: 70 × 50 mm. It employs a dual-core architecture comprising FPGA and ARM. The FPGA is responsible for generating sawtooth wave modulation of the DFB laser at a frequency of 100 KHz and facilitates rapid data acquisition from the photoelectric conversion circuit. On the other hand, the ARM processor ensures precise temperature control of the laser, maintaining accuracy within ± 0.1 °C, and conducts the computation of gas concentration. Fitting the standard gas concentration to the gas absorption signal amplitude demonstrates a strong linear correlation, with a correlation coefficient (R^2) of 0.998. Long-term concentration monitoring experiments reveal the sensor's superb stability, with a minimum detection limit of 43.14 ppm·m. Responsiveness experiments indicate a swift response time of 1.8 ms, allowing the sensor to rapidly respond to changes in gas concentration. Therefore, the methane telemetry sensor, with its high responsiveness, compact size, and open-circuit design, shows promising potential for wide-ranging applications such as in handheld telemetry devices, UAV gas detection systems, vehicle-mounted gas detection, and laser gas radar, amongst others.

Author Contributions: Conceptualization, Q.W. and B.Y.; methodology, Q.W.; software, Q.W.; validation, Q.W., W.W. and C.M.; formal analysis, Q.W.; investigation, Q.W.; resources, Q.W.; data curation, Q.W., Y.Y. and Y.X.; writing—original draft preparation, Q.W.; writing—review and editing, Q.W. and Y.S.; visualization, Q.W.; supervision, B.Y.; project administration, B.Y.; funding acquisition, B.Y. All authors have read and agreed to the published version of the manuscript.

Funding: This research was funded by Nanjing University of Aeronautics and Astronautics Human Resource Department talent startup funds (1005-YQR17020) and Central Guidance of Local Science and Technology Development funds (2023ZY1023).

Institutional Review Board Statement: Not applicable.

Informed Consent Statement: Not applicable.

Data Availability Statement: Data are contained within the article.

Conflicts of Interest: The authors declare no conflict of interest.

References

1. Huang, S.; Wang, B.A.; Chen, L.X.; Yu, Y.B.; Dai, T.X.; Lian, H.Q. Development of VCSEL laser detection system for methane gas. In Proceedings of the International Conference on Sensors and Instruments (ICSI), Qingdao, China, 28–30 May 2021; SPIE—International Society for Optics and Photonics: Baltimore, MD, USA, 2021.
2. Huang, Y.; Fu, W.; Yang, S.; Li, C.G.; Hu, X.W.; Zhang, M.R.; Chen, C.; Chang, S.P. Highly sensitive measurement of trace methane gas using mid-infrared tunable diode laser absorption spectroscopy method. *Microw. Opt. Technol. Lett.* **2023**, *5*. [[CrossRef](#)]
3. Wang, Z.M.; Wang, H.; Yu, Y.C.; Zhang, M.Y.; Ma, L.L.; Zou, F.; Wang, C.H.; Kang, J.J. Simulation and Analysis of CH₄ Concentration Measurement Based on QCL-TDLAS. In Proceedings of the 2nd Global Conference on Ecological Environment and Civil Engineering (GCEECE), Guangzhou, China, 7–9 August 2020; IOP Publishing Ltd.: Bristol, UK, 2020.
4. Dong, L.; Tittel, F.K.; Li, C.G.; Sanchez, N.P.; Wu, H.P.; Zheng, C.T.; Yu, Y.J.; Sampaolo, A.; Griffin, R.J. Compact TDLAS based sensor design using interband cascade lasers for mid-IR trace gas sensing. *Opt. Express* **2016**, *24*, A528–A535. [[CrossRef](#)]
5. Ziting, L.; Shunda, Q.; Yufei, M. Fabry–Perot-based phase demodulation of heterodyne light-induced thermoelastic spectroscopy. *Light Adv. Manuf.* **2023**, *4*, 23.
6. Zhang, C.; Qiao, S.D.; He, Y.; Zhou, S.; Qi, L.; Ma, Y.F. Differential quartz-enhanced photoacoustic spectroscopy. *Appl. Phys. Lett.* **2023**, *122*, 6. [[CrossRef](#)]
7. Witzel, O.; Klein, A.; Meffert, C.; Wagner, S.; Kaiser, S.; Schulz, C.; Ebert, V. VCSEL-based, high-speed, in situ TDLAS for in-cylinder water vapor measurements in IC engines. *Opt. Express* **2013**, *21*, 19951–19965. [[CrossRef](#)]
8. Liu, C.; Xu, L.J.; Chen, J.L.; Cao, Z.; Lin, Y.Z.; Cai, W.W. Development of a fan-beam TDLAS-based tomographic sensor for rapid imaging of temperature and gas concentration. *Opt. Express* **2015**, *23*, 22494–22511. [[CrossRef](#)]
9. Gong, W.; Zhang, Q.; Zhang, T.; Liu, T.; Wang, Z.; Wei, Y. Study on laser methane remote sensor based on TDLAS. In *AOPC 2022: Atmospheric and Environmental Optics*; SPIE: Bellingham, WA, USA, 2023; p. 125610A.

10. Witt, F.; Nwaboh, J.; Bohlius, H.; Lampert, A.; Ebert, V. Towards a Fast, Open-Path Laser Hygrometer for Airborne Eddy Covariance Measurements. *Appl. Sci.* **2021**, *11*, 10.
11. Sun, J.C.; Chang, J.; Wei, Y.B.; Zhang, Z.F.; Lin, S.; Wang, F.P.; Zhang, Q.D. Dual gas sensor with innovative signal analysis based on neural network. *Sens. Actuator B-Chem.* **2022**, *373*, 10. [[CrossRef](#)]
12. Lin, H.Z.; Wu, K.H.; Zhang, T.; Lai, X.M.; Mei, L. Remote sensing of vehicle emitted carbon oxides employing wavelength modulation spectroscopy and a segment modulation method. *Microw. Opt. Technol. Lett.* **2023**, *65*, 1162–1168. [[CrossRef](#)]
13. Lu, H.B.; Zheng, C.T.; Zhang, L.; Liu, Z.W.; Song, F.; Li, X.Y.; Zhang, Y.; Wang, Y.D. A Remote Sensor System Based on TDLAS Technique for Ammonia Leakage Monitoring. *Sensors* **2021**, *21*, 14.
14. Yang, H.Q.; Bu, X.Z.; Cao, Y.H.; Song, Y. A methane telemetry sensor based on near-infrared laser absorption spectroscopy. *Infrared Phys. Technol.* **2021**, *114*, 8.
15. Shen, S.Q.; Li, W.; Wang, M.J.; Wang, D.; Li, Y.S.; Li, D. Methane near-infrared laser remote detection under non-cooperative target condition based on harmonic waveform recognition. *Infrared Phys. Technol.* **2022**, *120*, 9. [[CrossRef](#)]
16. Li, G.L.; Ma, K.; Jiao, Y.; Jiang, Q.Z.; Zhang, X.N.; Zhang, Z.C.; Wu, Y.H.; Song, D. Performance enhancement of DFBL based near-infrared CH₄ telemetry system using a focus tunable lens. *Microw. Opt. Technol. Lett.* **2021**, *63*, 1147–1151. [[CrossRef](#)]
17. Li, Y.F.; Chang, L.; Zhao, Y.J.; Meng, X.J.; Wei, Y.B.; Wang, X.S.; Yue, J.H.; Liu, T.Y. A fiber optic methane sensor based on wavelength adaptive vertical cavity surface emitting laser without thermoelectric cooler. *Measurement* **2016**, *79*, 211–215. [[CrossRef](#)]
18. Raza, M.; Ma, L.H.; Yao, C.Y.; Yang, M.; Wang, Z.; Wang, Q.; Kan, R.F.; Ren, W. MHz-rate scanned-wavelength direct absorption spectroscopy using a distributed feedback diode laser at 2.3 μm . *Opt. Laser Technol.* **2020**, *130*, 6. [[CrossRef](#)]
19. Zhang, L.W.; Pang, T.; Zhang, Z.R.; Sun, P.S.; Xia, H.; Wu, B.; Guo, Q.; Sigrist, M.W.; Shu, C.M. A novel compact intrinsic safety full range Methane microprobe sensor using? trans-world? processing method based on near -infrared spectroscopy. *Sens. Actuator B-Chem.* **2021**, *334*, 7.
20. Dang, J.M.; Zhang, J.H.; Dong, X.J.; Kong, L.J.; Yu, H.Y. A trace CH₄ detection system based on DAS calibrated WMS technique. *Spectrochim. Acta A Mol. Biomol. Spectrosc.* **2022**, *266*, 7.
21. Sang, J.; Yang, X.Y.; He, T.B.; Li, J.S. High sensitive detection of atmospheric methane using infrared laser absorption spectroscopy. In Proceedings of the 14th National Conference on Laser Technology and Optoelectronics (LTO), Shanghai, China, 17–20 March 2019.
22. Zhang, T.T.; Zhang, L.; Li, Y.F.; Wei, Y.B.; Wang, Z.W.; Gong, W.H.; Lv, L.; Wang, J.Q.; Liu, T.Y. High Precision Detection Method of Methane in Extreme Environment based on TDLAS. In Proceedings of the 10th International Symposium on Advanced Optical Manufacturing and Testing Technologies-Intelligent Sensing Technologies and Applications, Chengdu, China, 14–17 June 2021.
23. Zhao, H.; Zheng, C.T.; Pi, M.Q.; Liang, L.; Song, F.; Zhang, Y.; Wang, Y.D.; Tittel, F.K. On-chip mid-infrared silicon-on-insulator waveguide methane sensor using two measurement schemes at 3.291 μm . *Front. Chem.* **2022**, *10*, 11. [[CrossRef](#)] [[PubMed](#)]
24. Burkle, S.; Walter, N.; Wagner, S. Laser-based measurements of pressure broadening and pressure shift coefficients of combustion-relevant absorption lines in the near-infrared region. *Appl. Phys. B-Lasers Opt.* **2018**, *124*, 12.
25. Tu, R.; Gu, J.Q.; Zeng, Y.; Zhou, X.J.; Yang, K.; Jing, J.J.; Miao, Z.H.; Yang, J.H. Development and Validation of a Tunable Diode Laser Absorption Spectroscopy System for Hot Gas Flow and Small-Scale Flame Measurement. *Sensors* **2022**, *22*, 14.
26. Li, B.; Zheng, C.T.; Liu, H.F.; He, Q.X.; Ye, W.L.; Zhang, Y.; Pan, J.Q.; Wang, Y.D. Development and measurement of a near-infrared CH₄ detection system using 1.654 μm wavelength-modulated diode laser and open reflective gas sensing probe. *Sens. Actuator B-Chem.* **2016**, *225*, 188–198. [[CrossRef](#)]
27. Wu, X.; Sang, J.; Zhou, S.; Li, J.S. High sensitivity open-path gas sensor based on a triangular multi-pass cell. *Microw. Opt. Technol. Lett.* **2021**, *63*, 2510–2516. [[CrossRef](#)]
28. Mohammad, I.L.; Anderson, G.T.; Chen, Y.H. Noise estimation technique to reduce the effects of 1/f noise in Open Path Tunable Diode Laser Absorption Spectrometry (OP-TDLAS). In Proceedings of the Conference on Sensors for Extreme Harsh Environments, Baltimore, MD, USA, 7–8 May 2014; SPIE—International Society for Optics and Photonics: Baltimore, MD, USA, 2014.

Disclaimer/Publisher’s Note: The statements, opinions and data contained in all publications are solely those of the individual author(s) and contributor(s) and not of MDPI and/or the editor(s). MDPI and/or the editor(s) disclaim responsibility for any injury to people or property resulting from any ideas, methods, instructions or products referred to in the content.